

1 Introduction

Earthquakes in subduction zone represent the largest part of seismic activity worldwide. Indeed, along subduction zones were sediments, oceanic crust and mantle lithosphere return and reequilibrate with earth's mantle, generally large and shallow earthquakes contribute about 90 % of the total seismic moment released (Stern, 2002).

Our understanding of the tectonic processes that occur along subduction zones is based on geological models representative of this specific geodynamic environment. This helps to explain three principal features: a deep ocean trench, a volcanic arc, on the overriding plate parallel to the trench, and a plane, defined by earthquakes, shallow near the trench and descending beneath and beyond the volcanic arc. However, due to the lack of information in particular on the deep structure of the subduction zone, some questions remain open. For example in an area like Lesser Antilles region what is the particular structural framework and kinematics of active margins?

For many subduction zones, the seismic activity can be monitored and investigated by regular seismometers deployed on land, thanks to the presence of the upper plate forearc that is sub-aerial there. This is the case on Shikoku and central Honshu islands for the Nankai-Tokai subductions where the young Philippine sea plate subducts. For Northern Honshu the subaerial part of the forearc domain reaches out 100 km from the volcanic arc axis. The slab top is at 45 km depth beneath the coastline. In contrast, in the Lesser Antilles, emerged land is narrow and thus observation of earthquakes with regular seismometer is limited to 25 km from the volcanic arc, where the slab already reaches 90 km depth. There is an exception for Guadeloupe archipelago with its eastern half of Grande Terre, prolonged by Désirade islet. This spur-like domain offers a 70 km wide domain from the volcanic arc, but still remains at a 200 km distance from the subduction deformation front. These conditions conducted us to use sea-bottom observations for the seismological study of forearc earthquake occurrence.

In this work, in order to study the relationship between tectonic structures and seismicity, we show results of the experiment SISMANTILLES I on the central Lesser Antilles Subduction Zone. We analyzed seismicity by using the data recorded by a temporary combined on- and offshore network and present a P- and S-wave first arrival time passive tomography. This investigation programme on Lesser Antilles arc, was carried out, in two phase, by « Laboratoire de sismologie expérimentale » of the « Institut de Physique du Globe de Paris » from November 1999 to January 2002.

The main objectives of this study are: to characterize the geometry of the subducted slab and to estimate the seismic activity linked to the dynamics of subduction. The results of a high precise earthquake location and of the 3-D travel time tomography provide important constraints on the structure and evolution of this subduction zone. MCS and WARR studies along 2-D profiles (Laigle et al., 2011) are also used for comparison and validation of the present study.

In the chapter, after a brief introduction of the geodynamical context of the Lesser Antilles region, the previous local earthquake studies will be summarized. Then will be described the concept of local earthquake tomography and the approach used for 1-D and 3-D inversions.

1.1 Tectonic settings of Lesser Antilles Arc

Along the Lesser Antilles Arc, the North American and Caribbean plates converge at a rate of about 2 cm/yr (DeMets et al., 2000).

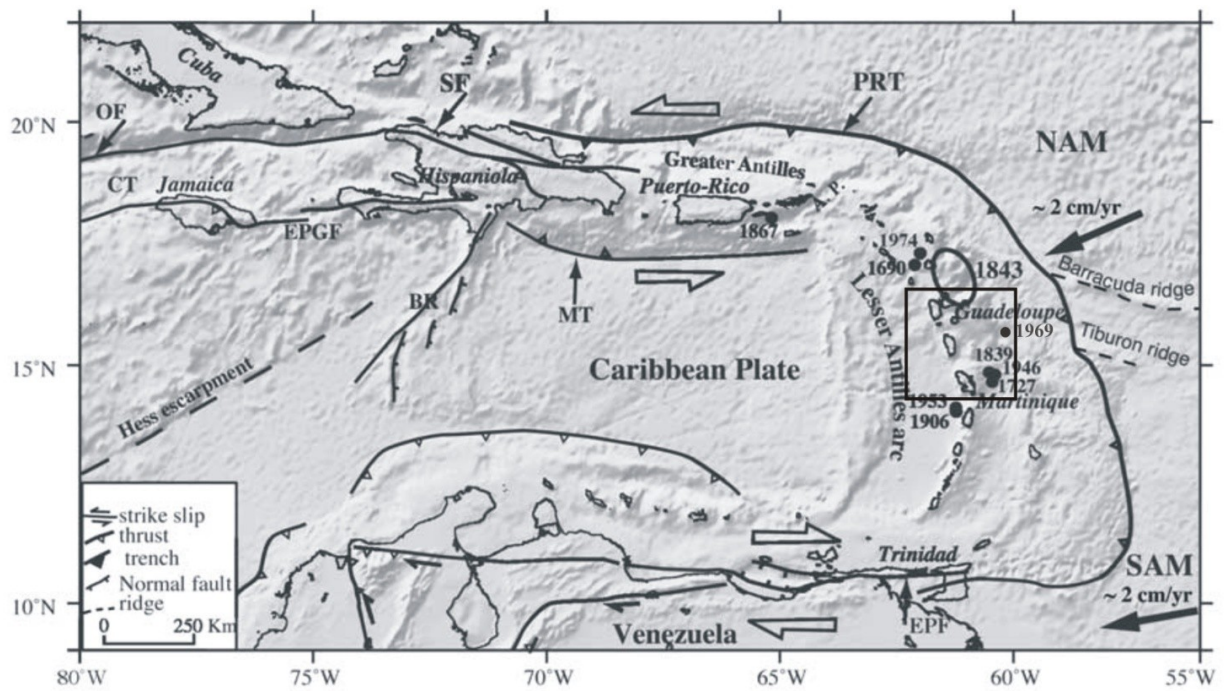


Figure 1.1: General setting of the Lesser Antilles Arc. Subduction rates from DeMets et al. (2000). CT: Cayman Trough, OF: Oriente Fault zone, EPGF: Enriquillo-Plantain Garden fault zone; BR: Beata Ridge; MT: Muertos trough, PRT: Puerto Rico trench, EPF: El Pilar Fault zone, NAM: North American Margin, SAM: South American Margin. Black circles: major historical earthquakes ($M > 7$) in the Lesser Antilles Arc. The patch ruptured by the 1843 earthquake is indicated. Box indicates studied area. Black dashed lines mark Barracuda (BR) and Tiburon ridges (TR) (Modified from Feuillet et al. 2002).

This motion (figure 1.1) is chiefly absorbed, in a roughly $S67^\circ$ direction, by subduction of Atlantic seafloor under beneath Caribbean plate that is responsible for active volcanism and regional earthquakes. The Caribbean Plate is bounded to the north by the North American-Caribbean plate boundary zone, a seismogenic zone with mainly left-lateral strike-slip deformation, and to the south by a dextral strike-slip fault zone. Therefore, our investigated subduction zone results strongly curved between these two strike-slip boundaries. The Lesser Antilles arc is a 850 km long island arc that extends submeridionally from the South American continent to the eastern termination of the Greater Antilles from which is separated from the Anegada passage (figure 1.2). It forms the eastern boundary of the Caribbean plate beneath which the Atlantic crust is subducted. This island arc has experienced a complex history and has probably been active since the Early Cretaceous (Bouysse et Westercamp, 1990). With the onset of the Eocene, a volcanic front settled upon this Mesozoic arc substratum. Its trace (figure 1.2 dashed black line) can be located from Martinique, in the south, to Anguilla, in the north, and constitutes the Older arc (early Eocene-middle Oligocene). This volcanic line later ceased its activity and, after several million years on early Miocene, the volcanism resumed along the Recent arc, which is still active today. This event has been interpreted as a consequence of the shallowing of the slab's dip after a buoyant Atlantic aseismic ridge collided to the margin. From Martinique northwards, the two arcs are separated by a passage about 50 km wide, the Kallinago depression (Bouysse et Westercamp, 1990).

These two northern branches (figure 1.2) have been also called the "Outer arc" to the east (from Marie Galante to Anguilla) and the "Inner arc" to the west (from Dominica to St. Kitts). The surface contact between the Caribbean plate and the subducted Atlantic crust is underlined by a strong negative gravity anomaly (Bowin, 1976). The distance between the present northern volcanic front and this anomaly is of about 250 km. Physiographically, this contact corresponds to a classical subduction trench (more than 6,000 m deep) only to the north of Antigua island and constitutes the southeastern extension of the Puerto Rico Trench (figure 1.2). To the south, the trench is progressively filled in by sediments and passes to the Barbados accretionary prism, which rises above sea level to form Barbados island.

The accretionary complex increases in its width to the south and shows a maximum thickness of 7 km south of $11^\circ N$. In this case sediments are mostly made of turbiditic material while north of the Barracuda ridge they form only a 200 m thin blanket that is essentially pelagic (Westbrook et al., 1988). This large change of sedimentary inputs is directly responsible for the variations in width and elevation of the Barbados complex, one of the best

examples of sedimentary accretionary prisms in the world that owes its importance to the huge longitudinal sedimentary input coming from the Orinoco and Amazon rivers (Moore et al., 1982).

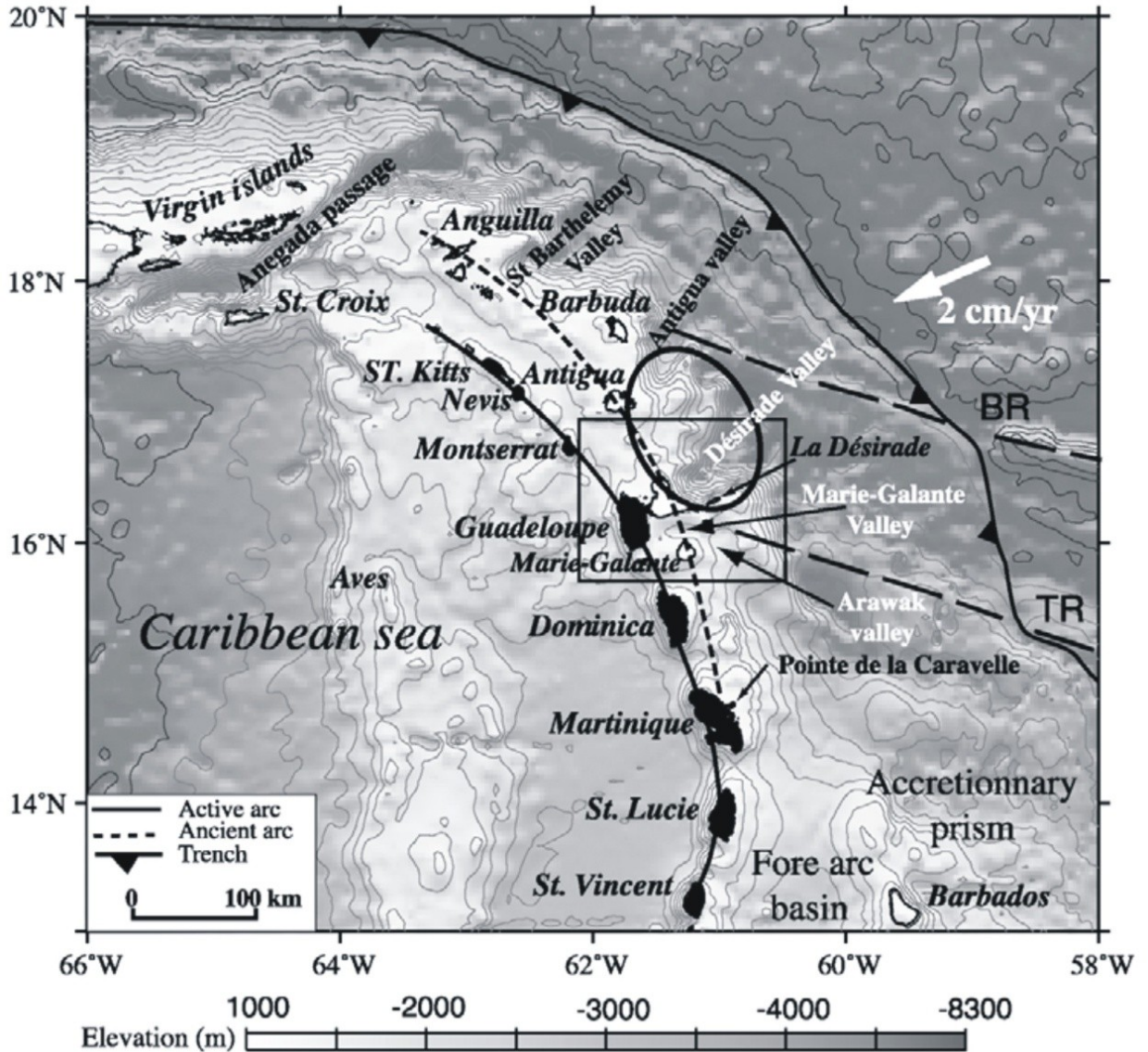


Figure 1.2: Map of Lesser Antilles arc modified from Feuillet et al. (2002). Bathymetry from Smith and Sandwell (1997), the isobath interval is 500 m. Continuous black line, recent volcanic arc; dotted black line, ancient arc. Volcanic islands (on recent arc) in black; coral reef islands (on ancient arc) in white. Box indicates studied area. Black dashed lines mark Barracuda (BR) and Tiburon ridges (TR). The deformation front (continuous line with triangles) marks the subduction of the Atlantic Ocean lithosphere beneath the Caribbean plate.

The Eastern Caribbean is, therefore, characterized by the consumption of the relatively old Cretaceous oceanic crust of the North American plate. The latter is cut by several fracture zones which in a sinistral sense, offset magnetic anomalies by an amount ranging from 60 to 250 km (Westbrook et al., 1988). To the east of the Barbados complex deformation front, the Atlantic crust does not show an uniform physiography. It is characterized by two WNW-ESE trending aseismic ridges that are the Barracuda and Tiburon Ridges (figures 1.1 and 1.2). Both ridges are uncompensated and likely formed of a thinned crust and uplifted mantle. They are usually interpreted as ridges associated to oceanic fracture zone of the Atlantic lithosphere (e.g., Stein et al., 1982). A shift of the deformation front of ~100 km is observed south of Dominica island and is linked to the Tiburon ridge subduction that acts as a barrier to northern sediment deposition. In fact, the forearc is ~250 km wide in the northern part of the Lesser Antilles arc and is ~450 km wide in the south where the Barbados accretionary prism is larger.

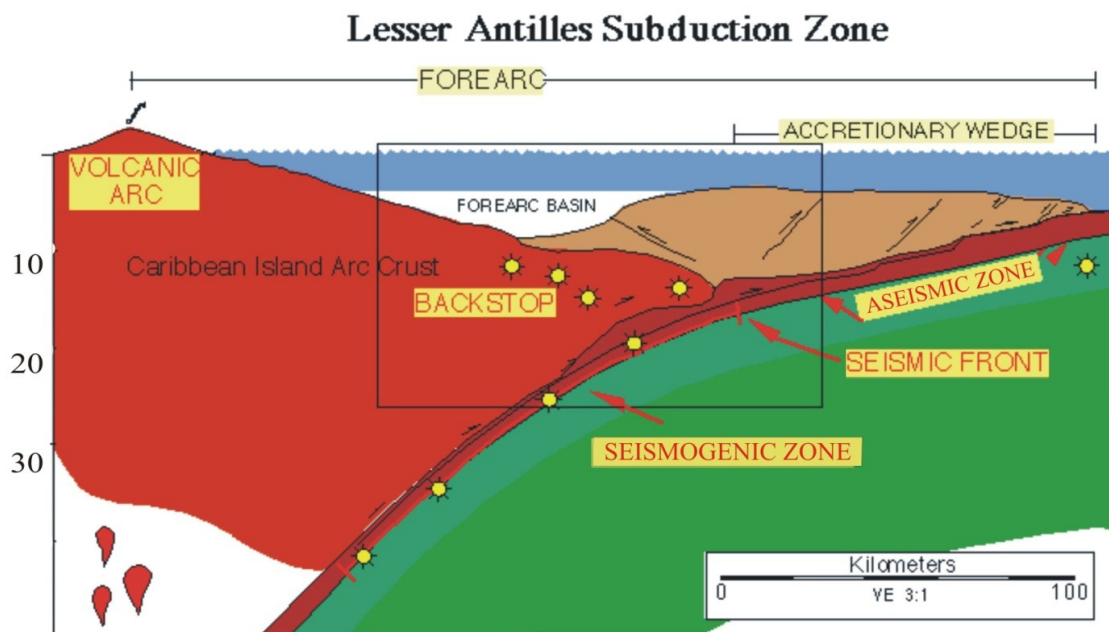


Figure 1.3: A schematic cross section of the Lesser Antilles subduction zone, where the oceanic crust of the North American Plate subducts beneath the Caribbean island arc crust. Sediments accumulated on the subducting North American crust (brown) are either accreted to the accretionary wedge at the toe (light brown) or are carried deeper (dark brown) beneath the accretionary wedge, or beneath the Caribbean island arc crust, or down the subduction zone to be melted deep in the mantle. Magmas generated by sediment melting erupt at the volcanic arc. Earthquakes are frequently generated along the seismogenic zone between 10 - 30 km depth. The

target area of the seismic imaging and structural analysis in this study is shown by the dashed-in box (modified from Byrne *et al.* 1988).

Before being absorbed by the subduction and underthrust beneath the overriding Caribbean plate, the above-mentioned ridges pass under the deformation front and the Barbados accretionary complex (Westbrook *et al.*, 1988). The upper part of the sedimentary column, overlying the Atlantic crust and located above zones of décollement, is accreted at the leading edge of the complex and, farther to the west, incorporated from beneath into the wedge complex. The lower part of the sediments is thought to be absorbed, undeformed, by the subduction zone, beneath the Caribbean plate (Fig. 1.3). With regard to the oceanic ridges, their sedimentary capping is probably scraped off and incorporated into the prism. The peeling should contribute to the enhancement of the contrast between the sedimented and non-sedimented areas of the subducted slab plunging into the asthenospheric wedge.

1.2 Previous constraints on the seismicity

The eastern edge of the Lesser Antilles arc is known as a region of high volcanic hazard. In 1902, for instance, the eruption of Mont Pelée resulted the worst volcanic disaster of 20th century. The eruption caused about 30,000 casualties and completely destroyed, at about 4 miles south of the peak of Mont Pelée, the town of Saint Pierre. But Lesser Antilles Arc is also a region where the seismic hazard is very high.

Historically, several large ($M > 7$) earthquakes have been recorded (Dorel, 1981). Two major earthquakes (5 April 1690 and 8 February 1843 occurred) north of Guadeloupe. Guadeloupe itself was also affected in 1851 and 1897 by two moderate earthquakes with intensities VII-VIII. Offshore Martinique different destructive and moderate earthquakes, with reported intensity between V to IX, occurred from 1702 to 1839. Dorel (1981) noted that most of seismic activity concentrates close to the island arc, 150-200 km westward of deformation front (Christeson *et al.*, 2003). The Christmas Day 1969 event of magnitude 6.4 and its aftershock sequence (offshore Dominica-Guadeloupe) is an exception. It is the most eastward recorded event of such magnitude due to the bending of the subducting plate (Dorel, 1981).

In the forearc, Girardin *et al.* (1991) suggested that shallow seismicity is related to deformation due to the subduction of Barracuda and Tiburon ridges. In the arc, the shallow seismicity is accommodating deformations in the Caribbean plate by normal and oblique faults (Stein *et al.*, 1982). An example is the November 2004, Mw 6.2 earthquake, that occurred in

“Les Saintes Archipelago”, between Guadeloupe and Dominica. The mainshock was followed by aftershock series that is still going on (Bazin et al., 2010).

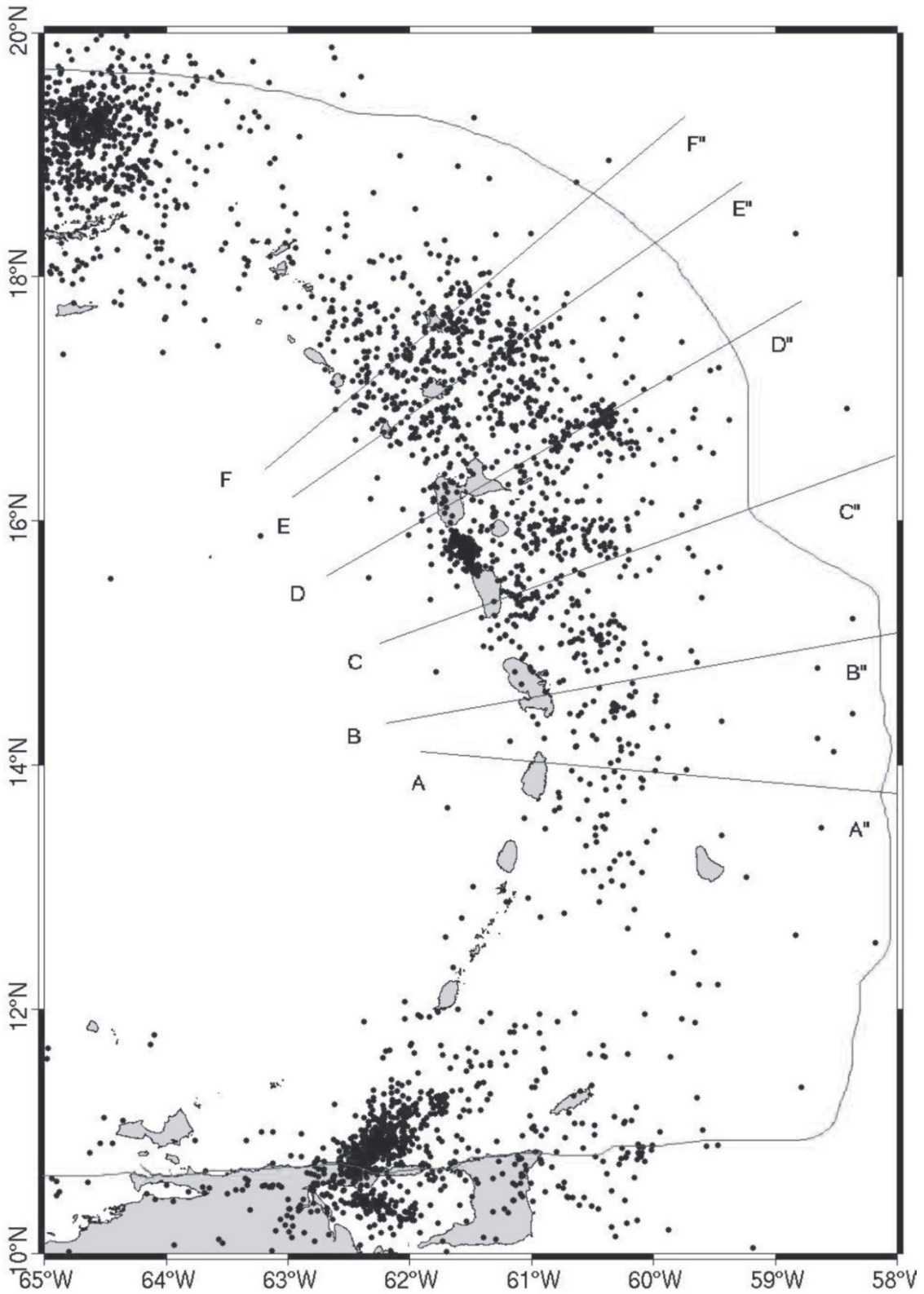


Figure 1.4: Seismicity map (2001-2005) of CDSA complete catalog for the Lesser Antilles region. Profiles AA", BB", CC", DD", EE" and FF" indicate the orientations of the cross-sections showed in Fig. 1.5. The continuous line represents the oceanic trench. Modified from Bengoubou et al. (2008)

Historical seismicity covers too short a period of time (less than three and one-half centuries) to estimate the recurrence time of strong events or their maximum magnitude. Indeed instrumental recording of earthquakes in the Lesser Antilles arc began in 1936 with the installation of the first permanent seismic station in Martinique (Dorel, 1981). This station was followed in 1947 by another on the island of Guadeloupe. In 1950 stations were set up on each main island by the seismic research unit of Trinidad. Finally, in 1973 a French telemetry network of nine stations was set up on the three islands of Martinique, Guadeloupe and Dominique. Figure 1.4 shows the epicentral map for the period January 2001 to May 2005 determined by the "Centre de Données Sismologiques des Antilles" (hereafter CDSA) in the Lesser Antilles arc between 10°-20° north and 58°-63° west. CDSA collects all available data from French West Indies arrays, centralizing them into a single database. The Center involves three institutions: the Observatoire volcanologique et sismologique de Guadeloupe (OVSG); the Bureau de Recherches Géologique et Minières (BRGM) ; the Université des Antilles et de la Guyane (UAG). For more details, please consult the website <http://www.seismes-antilles.fr>.

Earthquake locations were obtained using an approximate Earth structure determined by Dorel et al. (1974) along the arc. This crustal structure is characterized by a three-layers model: the compressional velocity is about 3.5 km s⁻¹ down to a depth of 3 km. Below this depth the velocity is 6.0 km s⁻¹ in a layer whose thickness is about 12 km. Under this layer the P- wave velocity is 7.0 and the layer thickness is 15 km. Finally the mantle, whose mean velocity has been taken to 8.0 km s⁻¹, underlies the crust. Considered as a whole, the seismicity level is rather low for an active margin, and is probably due to the slow convergence rate (ca. 2 cm/yr) (Stern, 2002). This value agrees with the relation of Ruff and Kanamori (1980) who found a relationship between the length of the seismic zone and the convergence rate for a subduction region.

Most of the seismicity occurs arc ward; Chen et al. (1982) suggest that no events occur within the prism near Barbados and that accretionary prisms are, in general, aseismic. A difference in seismicity, noted by Dorel (1981), occurs between the northern (north of 14°N) and southern portions of the arc. The southern region is substantially less active than the northern one and the deepest seismicity is concentrated in the area between Martinique and Dominica (figure 1.5). This area was the epicentral zone of the February 1906 M=7.5 and

November 2007 Mw 7.4 event, both of them occurred at depths greater than 100 km. Also, before the deployment of global seismic networks at the beginning of the 60s, thrust events at intermediate depths and related with the seismogenic zone are also been reported in the zone as the February 1843 (Bernard et Lambert, 1988). The dipping zone of seismic activity associated with subduction may be presented by vertical cross-sections along the arc. Figure 1.5 shows six cross-sections along profiles of figure 1.4. The sections are 100 km wide. From this earthquake distribution we try to draw the boundary of the plates and the shape of the slab. But this is difficult because of crustal seismicity and hypocentral uncertainties whose consequence in the scattering of the focus (see paragraph 2.4).

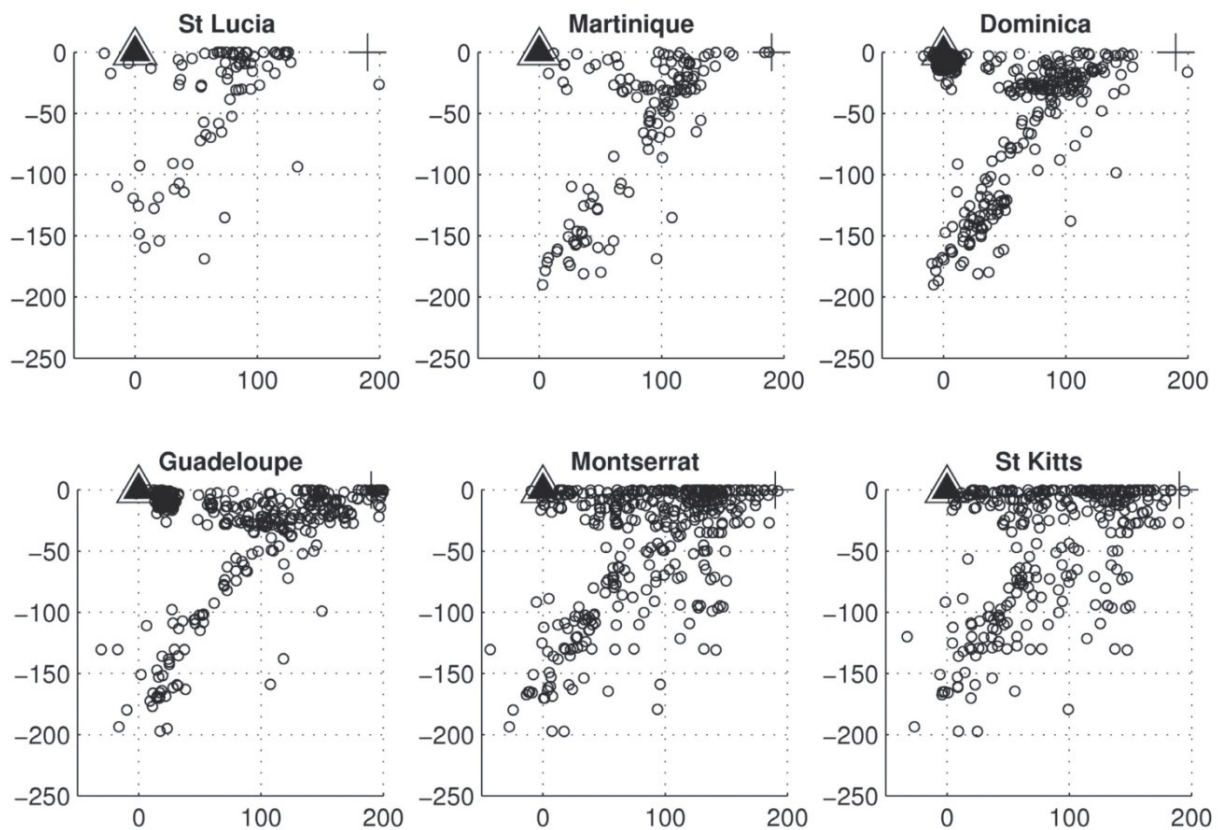


Figure 1.5: Seismicity cross-sections for six profiles perpendicular to the arc, trough active volcanic islands (AA'' to FF'' shown in Fig. 1.4). The sections are 150 km wide. Triangles on the horizontal axis indicate the active volcanic front. Modified from Bengoubou et al. (2008)

The distribution of events with depth seen on the different cross-sections show a relatively fairly well defined Benioff zone. The cross-sections from FF'' in the north to AA'' in the south give an angle of about 45° . Little variations of the dip of the slab may be related to the

transformation of movement from a pure subduction in the center of arc to a transform trench fault zone in the north and a transform strike-slip fault zone in the south (Stein *et al.*, 1982). In the Lesser Antilles Arc before SISMANLILLES I survey, seismic reflection experiments were mainly concentrated on the structure of the forearc and accretionary prism. They demonstrate the presence of a decollement beneath the accretionary prism (Westbrook, 1982) (figures 1.6). The contact between the fore-arc crust and the diving oceanic crust has been identified thanks to the strongly folded reflectors over the backstop.

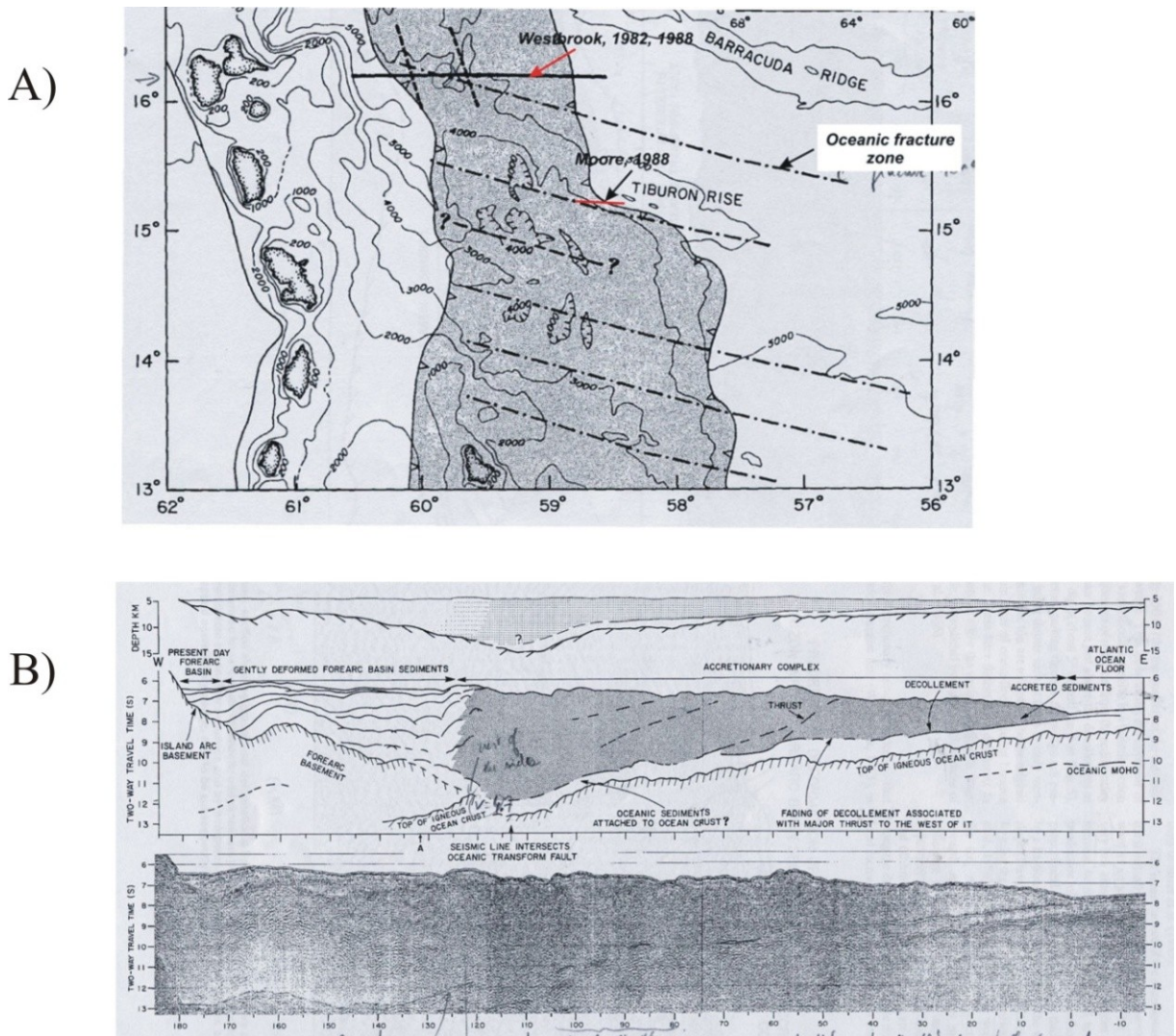


Figure 1.6: a) Position map of the seismic lines (Westbrook, 1982, 1988) and the drillings (Moore et al., 1982) realized on the accretionary complex of the Lesser Antilles b) The seismic section and corresponding interpretation through the accretionary complex of Barbados, (Westbrook, 1988).

Another seismic reflection, refraction acquisition has been carried out in 1998 with N/O M. Ewing (Bangs et al., 2003 and Christeson et al., 2003). A total number of 8 MCS lines parallel to the arc and 4 perpendicular lines have been allowed a penetration down to 10 km beneath the sea-floor (figures 1.7) A mapping of backstop topography outline has been obtained.

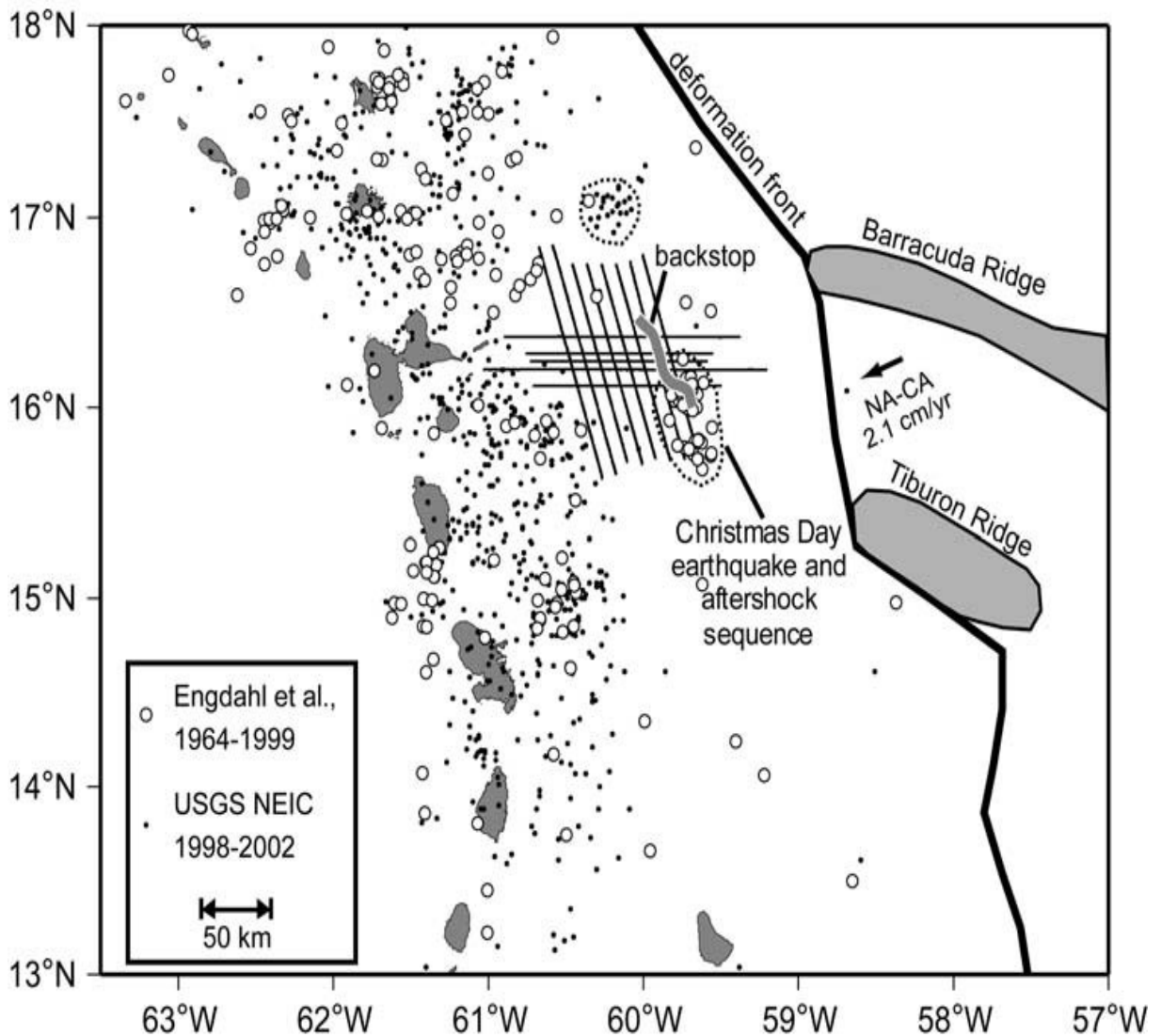


Figure 1.7: Position map of the seismic reflection/refraction survey with R/V M. Ewing (From Christeson et al., 2003). Seismicity from Engdahl et al. database (1998); earthquakes from the USGS NEIC database are plotted for the 5-year period 1998-2002. Two earthquake clusters are shown by the dotted lines.

1.3 Theory of Local Earthquake Tomography (LET)

Seismic tomography is a technique for three-dimensional images of the earth structure deriving from a large set of observations made at the periphery of a targeted earth volume. Using this technique arrival times of a dense set of rays crossing and sampling this volume are used to locate velocity anomalies in space.

If compared with controlled-source tomography, the use of local earthquake as sources for seismic tomography has both advantages and disadvantages. The advantages of local earthquakes compared with controlled sources are their substantial excitation of both compressional and shear waves and their three-dimensional spatial distribution. However, these advantages are diminished by both the lack of control on their distribution and on independent knowledge of their exact individual locations and origin times. Besides, the depth extent of models derived from local earthquake tomography (hereafter LET) will be limited by the maximum earthquake focal depths in the area.

The landmark paper by Aki and Lee (1976) can be regarded as the start LET. Since then, several numbers of books, papers and Ph.D. theses have been devoted to the inversion of local travel time data. Good introductions to the field of local earthquake tomography can be found in Kissling (1988) and Thurber (1993). The goal of this paragraph is to present the basic theory of LET.

The body wave travel time T from an earthquake i to a seismic station j is expressed using ray theory as a path integral

$$T_{ij} = \int_{source}^{receiver} u \, ds, \quad (1)$$

Where u is the slowness field (reciprocal of velocity) and ds is an element of path length. The actual observations are the arrival times t_{ij} , where

$$t_{ij} = \tau_i + T_{ij}, \quad (2)$$

and τ_i is the earthquake origin time. In a sense, the only knowns in the LET problem are the receiver locations and the observed arrival times. The source coordinates (x, y, z) , origin times, ray-paths and the velocity field are unknown. The problem is indicated schematically in the following figure:

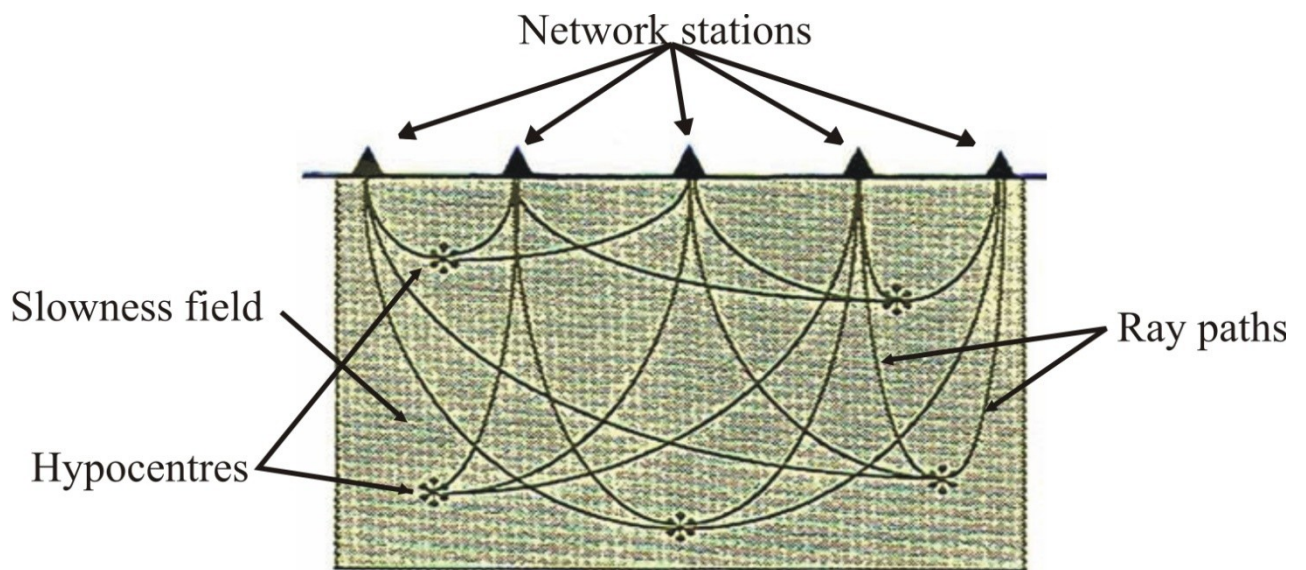


Figure 1.8: Schematic representation of the local earthquake tomography (LET) problem. A seismic network covers the area of geologic interest; earthquakes are distributed within the model volume. (Modified from Thurber, 1983)

Given a set of arrival times t_{obs} measured at a network of stations, the calculated arrival times t_{cal} are determined from equations (1) and (2) using trial hypocenters and origin times, and an initial model of the seismic velocity structure derived from the a priori information. The difference between observed and calculated arrival times are the residuals r :

$$r = t_{\text{obs}} - t_{\text{cal}}, \quad (3)$$

The goal of LET is to improve the estimates of the model parameters (velocity and hypocenters) by perturbing them in order to minimize the residuals values.

All LET methods are based on differing treatments of the following aspects of the problem:

- a) the scheme for the representation of the velocity structure;
- b) ray path and travel time calculation;
- c) the treatment of the hypocenter-velocity structure coupling;
- d) inversion methods;
- e) the assessment of solution quality;
- f) the use of S waves.

A) Representation of the velocity structure.

The choice of a particular parameterisation for the slowness field depends on the objectives of the tomographic analysis, particularly on the geometric features of the objects that are to be

described. Indeed the earth's crust has heterogeneous structure including complications such as discontinuities, faults, layering, intrusions, inclusions, zones of high temperature or partial melt and others random geologic heterogeneities.

In this section I will give a description of the different approaches of the model parameterization (Fig. 1.9).

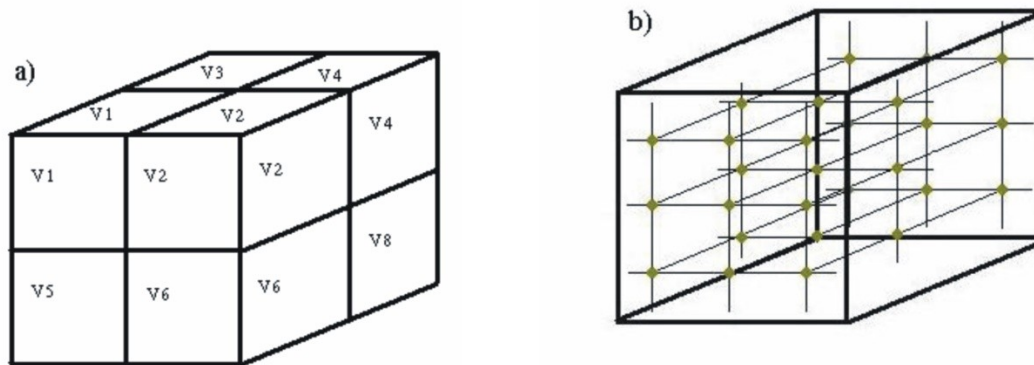


Figure 1.9: Schematic indication of two approaches to discrete velocity model representation: constant-velocity blocks (from Aki and Lee) and a grid of nodes (from Thurber). Dashed lines indicate the spatial form of interpolation. (Modified from Thurber, 1983).

There are two ways to describe the velocity structure of the Earth, which is to be determined by seismic tomography: one way by continuous functions, the second by a finite number of discrete parameters. Most seismic tomography techniques use the second approach. Popular parameterisation schemes are the use of the 3-D blocks and of the 3-D grid points (Fig. 1.9). In the first case, the velocity anomalies are within the subdivided 3-blocks while in the latter velocities are computed at grid points. In this context no single scheme can represent faithfully all aspects of this heterogeneity. The constant-velocity block approach of Aki and Lee (1976) treats the Earth as a set of boxes within each of which the seismic velocity is constant (Figure 1.7a). This approach has the advantage of simplicity, but it is clearly lacking in the ability to represent heterogeneous structures, even if these structures are as simple as slight gradients in the velocity or oblique discontinuities.

The need to especially define a velocity model during the forward calculation by a numerical grid, to adequately incorporate a priori information and to account for the variable data density, lead to the introduction of a three-grid approach. Thurber (1983) used a 3-D grid approach, in which velocities vary in all directions, with linear interpolation among nodes. An example of a seismic grid is the model parameterisation in widely used Simulps program (Thurber, 1983; Eberhart-Philips, 1986). The seismic grid is also the basis for later

display tomographic results. In the case of the SISMANTILLES I data set we prefer the interpolative method of Thurber for two reasons: (1) the velocity model representation is general and does not assume a specific geometry of structural heterogeneity; (2) the algorithm is suited to the scale of our problem, being capable of imaging anomalous bodies with characteristic dimensions of the order of ten kilometres or more.

B) Ray path and travel times calculation.

One of the problems that have to be solved in the LET method is the determination of the path of the seismic waves between each source-receiver pair and the travel time wave along that path. The travel time is needed to calculate the arrival time residual; the path is needed for computation of the hypocenter and velocity model. There are many techniques for determining ray-paths and travel time. These methods can be categorized as either exact or approximate, and the computational strategy involved usually can be classified as either shooting or bending. The use of approximate ray-tracing methods has the advantage of computational speed, but it introduces errors in the computation of residuals, hypocenter and velocity model because the travel time and the ray direction at the source will both be in error and the ray-path itself will not be correct. However, with the increasing power of modern computers, the use of overly simple ray-tracing is vanishing. Ray tracing is a two-points boundary value problem: the end-points specified (the source and the receiver positions) and the propagation path and time must be determined. Shooting methods solve the two points problem by iteratively solving an initial value problem with one fixed end-point and the initial ray trajectory varied (Fig. 1.10A). The bending method of ray tracing operates by adjusting the geometry of an initial arbitrary path that joins the source and receiver (Fig. 1.10B) until it satisfies Fermat's principle. The bending method proposed by Julian and Gubbins (1977) is designed for a continuous 3-D velocity medium and locates a two-point ray path by solving a system of first-order differential equations.

Um and Thurber (1987) develop a pseudo-bending technique for solving the two-point problem in continuous 3-D media. Their method is based on a perturbation scheme in which the integration step size is progressively halved. The initial guess path is defined by three points which are linearly interpolated. The centre point is then iteratively perturbed using a geometric interpretation of the ray equation until the extreme travel time converges within a specified limit, at which point the ray equation will be approximately satisfied. The number of path segments is then doubled and the three-point perturbation scheme is repeated working from both endpoints to the middle. The number of segments is doubled again and the

procedure is repeated iteratively (Fig. 1.10C) until the change in the travel-time between successive iterations satisfies some convergence criterion. In this work, among ray tracing techniques, the pseudo-bending method of Um et Thurber (1987) is used.

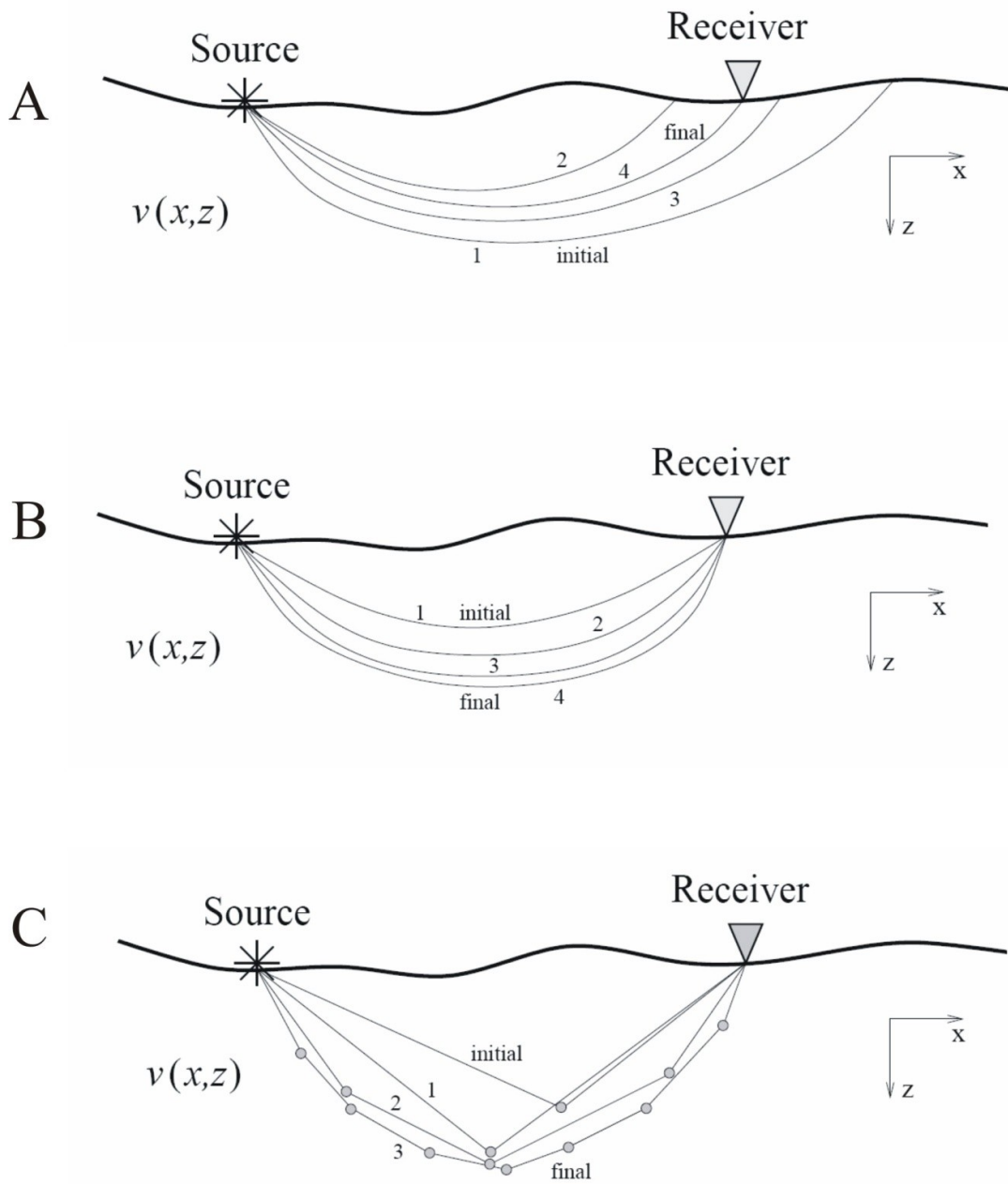


Figure 1.10: Representation of three approaches to ray-tracing. (A) shooting: the initial projection angle of ray 1 is iteratively adjusted until the final ray passes sufficiently close to the receiver. (B) bending: The geometry of the initial path is adjusted until it satisfies Fermat's principle. (C) pseudo-bending: An initial guess ray defined by

three points is provided. The centre point is perturbed to best satisfy the ray equation. Then the number of segments is doubled and the process is repeated. (Modified from Thurber, 1983).

C) *The treatment of the hypocenter-velocity structure coupling.*

Traditionally, the term “local earthquake tomography” has usually implied the determination of 3-D velocity structure keeping hypocenter parameters fixed at their initial values, while “simultaneous” inversion is usually construed to mean an explicit treatment of the hypocenter-velocity structure coupling. In this work, where the direct treatment of hypocenter-velocity structure coupling is required, an immediate concern is the growth of the matrix for the resolution of the problem. For a data set and model of L stations, N earthquakes and M velocity parameters, the construction of a matrix of size approximately $(L \times N)$ by $(4N + M)$ is implied. Even for a modest-sized inversion problem, with few stations, events and model parameters, the matrix size becomes formidable.

D) *Inversion methods.*

The LET inversion problem can become intractable due to the large size of the matrix involved. As computers become increasingly powerful, direct solution of full matrix inversion via Singular Value Decomposition (hereafter SVD) may become useful for very large problems (Lawson et Hanson, 1974). SVD avoids full matrix inversion, breaking down the matrix composed of the coefficients of the parameter derivatives into a product of three-orthogonal matrices containing the singular vectors of the data, model spaces and the corresponding singular values.

SVD is the approach applied in this work

E) *The assessment of solution quality.*

A 3-D model of structure derived from LET can be interpreted if its quality is known. Some measures of quality are “data variance reduction” and “model resolution”. “Data variance reduction” or “misfit” is a measure of the norm of the residual vector. “Model resolution” represents the interdependence of the model parameters. “Misfit” and “model resolution” are inherently coupled. In fact, it is well known that increasing the number of model parameters generally will diminishes the “misfit”. A model that is spatially finer in scale will be able to represent a structure at a higher spatial resolution, but the resolution of the individual model parameters will be reduced, once given the same set of data. In this study, examining the

output files of the code SIMULPS14, with data variance and model resolution, assesses an evaluation of inversion quality,

F) *The use of S waves.*

A more complete characterization of the mechanical properties and geologic identity of crust materials can be obtained from knowledge of the combination of P and S wave velocity structure. In this work, because we have many three-component data, we inverted also S-wave observations.

1.4 The approach for the 1-D and 3-D inversions

The approach used here for the simultaneous inversion of velocity structures and of hypocenter parameters was conceived on the basis of the “recipe” of Kissling *et al.* (1994). It is also possible to refer to the following sources: Kissling (1988); Kissling et Spackman (1996); Thurber (1983) and Eberhart-Philips (1986). This approach can be divided into three steps.

1. Checking of summary cards, localization and selection of best events. An a priori 1-D model is introduced.
2. 1-D inversion of travel time residual, in order to constrain a better tabular model. This model is called *1-D minimum model*.
3. 3-D inversion of residuals starting from the *1-D minimum model*.
 - During the first step, the code VELEST in “single-event mode” (Kissling, 1995) routinely relocates the events using the a-priori 1-D models. Then, the relocated events are selected following the control parameters chosen by the operator. Not only does this step computes a-priori hypocenter parameters used by the second step, but it also analyses the quality of phases through statistics.
 - During the second step, an 1-D inversion is performed to compute simultaneously hypocenter parameters, 1-D velocity model and station delays using the *best events*. The aim of this step is to constrain the best 1-D velocity model that will be used for 3-D inversion. This *1-D minimum model* should constrain hypocenter parameters that give the global minimum of the cost function. This function is the norm, in a least squares sense, of a weighted sum of the data misfit and an estimate of the complexity of the model. The 1-D inversion is performed by VELEST that run in a *simultaneous mode*. The 1-D

inversion is based on the same formalism than the one used by the 3-D inversion. The search for this best 1-D model may be a long process depending on the quality of the data and on the *goodness* of the a-priori knowledge one has about the investigation volume. Once the *1-D minimum model* is computed, the events are relocated once more using the new 1-D model and the original phases. If the new 1-D velocity model is not satisfactory, the *1-D minimum model* is not yet reached and the step has to be run again.

- The last step performs the 3-D inversion with the *best events* starting from the *1-D minimum model*. The program, named SIMULPS14, inverts for V_p using t_p travel times and (or) for V_p/V_s using S-P times. This program was originally written by C. Thurber as part of his thesis (Thurber, 1981). The formalism is based on a damped least squares minimization of the misfit function and on a full matrix inversion (see Thurber, 1993 and Eberhart-Phillips, 1993). The program can also invert for shots or blasts and can create synthetic travel time. Refer to the *user's guide* (Evans *et al.*, 1994) for more information and references. The Figure 1.9 summarizes the 3 steps.

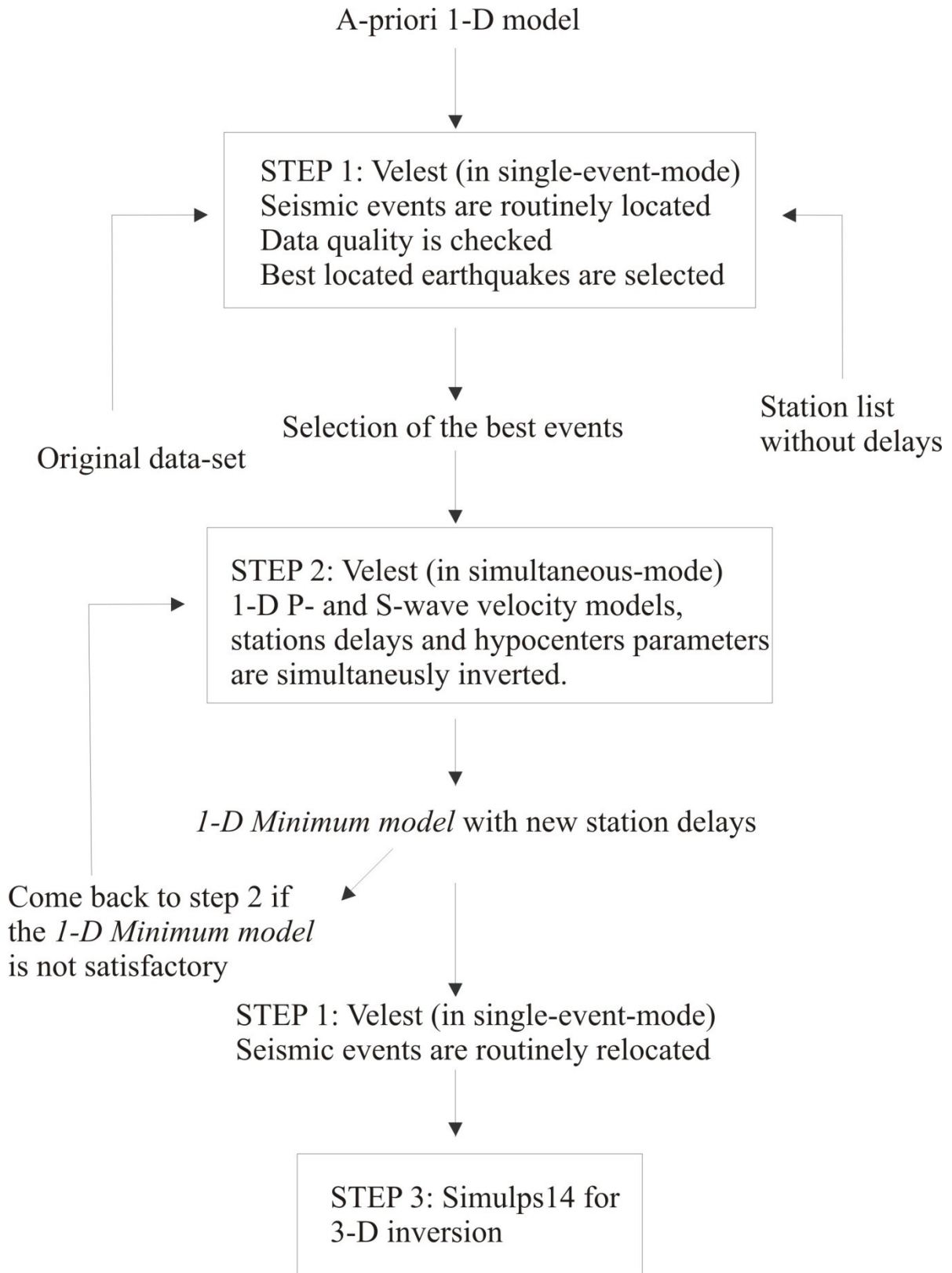


Figure 1.11: Three steps for 3-D tomography with local earthquakes.